

# Finite Element Analysis of Corner-Supported Composite Skewed Hypar Shell Roof Impacted by a Solid Striker

Sanjoy Das Neogi<sup>\*1</sup>, Amit Karmakar<sup>2</sup>, Dipankar Chakravorty<sup>3</sup>

1. Civil Engineering Department, Meghnad Saha Institute of Technology, Kolkata-700107, India

2. Mechanical Engineering Department, Jadavpur University, Kolkata-700032, India

3. Civil Engineering Department, Jadavpur University, Kolkata-700032, India

## Abstract

*Hyperbolic paraboloid shell is a preferred roofing unit in many practical situations demanding large column free spaces. Laminated composite has become a natural choice of different industrial sectors for its huge specific strength, specific weight, and good weathering resistance, is now being used by civil engineers too. The low transverse shear strength under the action of impact load prompted the researchers to study the response of the composite shells under such loads. Shells on point supports have wide applications in car parks and theatres etc. In the present study, a finite element code is applied to investigate the impact induced response of point-supported laminated composite hypar shells for different impact velocities. Contact behavior is described by modified Hertzian contact law and time dependent equations are solved using Newmark's method in present analysis.*

## 1. Introduction

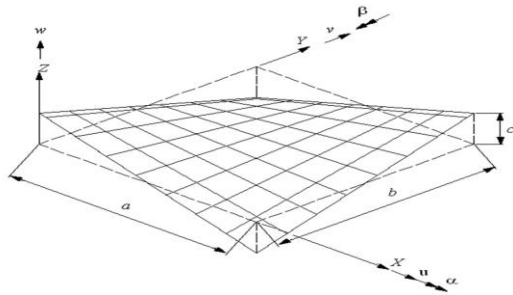
Hyperbolic paraboloid shell bounded by straight edges (commonly called hypar shell) is aesthetically elegant, easy to fabricate, being a doubly ruled surface and is preferred as roofing units in many practical situations demanding large column free space. In civil engineering applications of hypar shells as a roofing unit, their direct discrete support on columns is often needed. Car parks and theatres, where beams are normally absent in view of headroom restriction, often require large-span shell roofs supported on point supports. Moreover beams are sometimes undesirable in theatres from the viewpoint of the acoustics also. Introduction of laminated composite as an improved material, from the second half of the last century, in different branches of technology including civil engineering have prompted the researchers to study the different aspects of laminated composite hypar shells. In spite of the different advantages laminated composites are found to be vulnerable to sudden impact due to its low transverse shear capacity. It is obvious that an accurate modeling of contact behavior of target as well as the striker is the most important part of impact analysis. The classical contact law between elastic solids derived by Hertz [1] was found to be insufficient for composite materials and was modified

by Tan and Sun [2]. Time histories of contact force and displacement were reported by Sun and Chen [3] for simply supported initially stressed plate under impact using steel ball as an impactor. Impact analysis of shell structure was first reported by Toh et al.[4] for an orthotropic laminated cylindrical shell under low-velocity impact generated by a solid striker. Shim et al.[5] studied an elastic response of glass/epoxy-laminated composite ogival shells subjected to low velocity impact at any arbitrary location by a solid striker. They reported an analytic bi-harmonic polynomial solution. A finite element model, with and without geometric non-linearity, was presented by Kistler and Waas [6] for a laminated composite cylindrical shell subjected to transverse central impact. A parametric study of impact response and the resulting damage of laminated composite shell impacted by a metallic impactor were studied using finite-element method and Fourier series by Krishnamurthy et al.[7] for cylindrical curved panel. Karmakar et al.[8,9] undertook a transient dynamic finite element analysis to study the response of centrally impacted delaminated composite pretwisted cylindrical shells and rotating cylindrical shells due to low-velocity impact. Effects of transverse shear deformation and rotary inertia were included in their study. Based on the elastoplastic mechanics, the damage analysis and dynamic response of elastoplastic laminated composite shallow spherical shell of orthotropic material under low-velocity impact were studied by Yiming et al.[10] Laminated composites which are now often used as a roofing component in different shell forms by civil engineers, often subjected to impact load by wind born debris, snow-fall and in many other situations. These impacts cause hidden injury in the composites and may lead to total collapse due to gradual loss of stiffness. A close look through the literature shows the impact analysis of civil engineering shell forms are not addressed properly. A parallel review in the area of composite shells reveal that the industrially important hypar shells (Fig-1) need more in-depth study although some important aspects of these shell forms were reported recently by Sahoo and Chakravorty [11,12]. The only paper reported on impact response of composite hypar shells was due to Neogi et.al.[13] where they discussed

some aspects of such response of two-layered shells for simply supported boundary condition. But the impact analysis for point supported hypar remained untouched. Keeping in mind the industrial requirements, the impact response of point-supported composite hypar shells has been chosen for investigation in the present research.

## 2. Mathematical formulation

The basic mass and stiffness matrices of the skewed hypar shell (Fig-1) adopted in the present paper follows the equations and relations as reported by Sahoo and Chakravorty[11,12].



$$\text{Surface equation: } z = \frac{4c}{ab}(x - a/2)(y - b/2)$$

**Figure-1 Surface of a skewed hypar shell and degrees of freedom**

The dynamic equilibrium equation of the target shell for low velocity impact is given by the following equation:

$$\text{equation: } [M] \left\{ \ddot{\delta} \right\} + [K] \left\{ \delta \right\} = \left\{ F \right\} \quad (1)$$

where [M] and [K] are global mass and elastic stiffness matrices, respectively.  $\{\delta\}$  is the global displacement vector. For the impact problem,  $\{F\}$  is given as

$$\{F\} = \{0 \ 0 \ 0 \ \dots \ F_c \ \dots \ 0 \ 0 \ 0\}^T \quad (2)$$

Here  $F_c$  is the contact force given by the indentation law and the equation of motion of the rigid impactor is given as:

$$m_i \ddot{\omega}_i + F_c = 0 \quad (3)$$

where  $m_i$  and  $\ddot{\omega}_i$  are the mass and acceleration of the impactor respectively. Evaluation of the contact force depends on a contact law which relates the contact force with indentation. A power law was proposed by Yang and Sun [14] based on static indentation tests using steel ball as an indenter. This

contact law accounted the permanent indentation after unloading cycle i.e. collisions upon the rebound of the target structure after the first period of contact were considered. The modified version of the above mentioned contact law was proposed by Tan and Sun [2] was utilised by Sun and Chen [3]. The contact force model following Sun and Chen [3] is incorporated in the present finite element formulation. If  $k$  is the contact stiffness and  $\alpha_m$  is the maximum local indentation, the contact force  $F_c$  during loading is given by

$$F_c = k\alpha^{1.5} \quad 0 < \alpha \leq \alpha_m \quad (4)$$

The indentation parameter  $\alpha$  depends on the difference of the displacements of the impactor and the target structure at any instant of time, and so also the contact force. The values of  $\alpha$  are changing with time because of time varying displacements of both the rigid impactor and the target structure. At an instant the maximum indentation takes place and as a result maximum contact force is also obtained. At this instant displacement of the impactor also attains the maximum value (Goldmith, W.)[15]. There after the displacement of the impactor gradually decreases, but the target point displacement keeps on changing and finally increases to a maximum value and some point of time these two displacements become equal (Goldmith, W.)[15]. This leads to zero value of indentation and eventually the contact force becomes zero. At this instant the impactor loses the contact with the target. The process after attaining the maximum contact force till the reduction of contact force to zero value is essentially referred as unloading [3]. If the mass of the impactor is not very small, a second impact may occur upon the rebound of the target structure leading to a same phenomenon of contact deformation and attainment of maximum contact force. This process is known as reloading. If  $F_m$  is the maximum contact force at the beginning of unloading and  $\alpha_m$  is the maximum indentation during loading, the contact force  $F_c$  for unloading and reloading are expressed as [3].

$$\text{Unloading phase: } F_c = F_m \left[ \frac{\alpha - \alpha_0}{\alpha_m - \alpha_0} \right]^{2.5} \quad (5)$$

$$\text{Reloading phase: } F_c = F_m \left[ \frac{\alpha - \alpha_0}{\alpha_m - \alpha_0} \right]^{1.5} \quad (6)$$

where  $\alpha_0$  denotes the permanent indentation in a loading-unloading cycle.

$$\alpha_0 = \beta_c (\alpha_m - \alpha_p) \quad \text{if } \alpha_m > \alpha_{cr} \quad (7)$$

$$\alpha_0 = 0 \quad \text{if } \alpha_m < \alpha_{cr} \quad (8)$$

where  $\beta_c$  is a material dependent constant and  $\alpha_{cr}$  is the critical indentation beyond which permanent

indentation occurs, and the values are 0.094 and .01667cm respectively for graphite-epoxy composite (Sun and Chen 1985). Equations (1) and (3) are solved using Newmark constant- acceleration time integration

algorithm in the present analysis. Equation (1) may be expressed in iteration form at each time step.

**Table-1** Non dimensional natural frequencies  $\omega$  for three layer graphite epoxy twisted plates  $\psi/\theta/\theta$

Angle of twist	$\theta$ (deg)	0	15	30	45	60	75	90
$\phi = 15^\circ$	Qatu and Lessia[16]	1.0035	0.9296	0.7465	0.5286	0.3545	0.2723	0.2555
	Present formulation	0.9990	0.9257	0.7445	0.5279	0.3542	0.2720	0.2551
$\phi = 30^\circ$	Qatu and Lessia[16]	0.9566	0.8914	0.7205	0.5149	0.3443	0.2606	0.2436
	Present formulation	0.9490	0.8842	0.7181	0.5142	0.3447	0.2613	0.2444

$E_{11}= 138 \text{ GPa}, E_{22}=8.96 \text{ GPa}, G_{12} = 7.1\text{GPa}, \nu_{12} = 0.3: a/b = 1, a/h = 100$

$$[\bar{K}] \{ \bar{u}_{t+\Delta t} \} = \frac{\Delta t^2}{4} \{ \bar{R}_{t+\Delta t} \} + \{ \bar{M} \} \{ \bar{b}_t \} \quad (9)$$

Where

$$[\bar{K}] = \frac{\Delta t^2}{4} [\bar{K}] + [\bar{M}] \quad (10)$$

$$\{ \bar{b}_t \} = \{ \bar{R}_t \} + \Delta t \{ \dot{\bar{u}}_t \} + \frac{\Delta t^2}{4} \{ \ddot{\bar{u}}_t \} \quad (11)$$

The same solution scheme is also utilized for solving the equation of motion of the impactor, i.e. Equation (3). In Equation (9),  $i$  is the number of iterations within a time step. It is to be noted that a modified contact force  $F_{t+\Delta t}^i$  obtained from the previous

iteration is used to solve the current response  $\{ \bar{u}_{t+\Delta t} \}$ . The iteration procedure is continued until the equilibrium criterion is met.

### 3. Numerical example

Problems are solved with two different objectives. The present formulation is applied to solve natural frequencies of graphite-epoxy twisted plates, for problems appearing in published literature which are structurally similar to skewed hypar shells. This problem is expected to validate both the stiffness and mass matrix formulation of present finite element code. Another problem, solved earlier by Sun and Chen[3] regarding the impact response of composite plate, is taken up as the second benchmark to validate the impact formulation. The details of the benchmark problems are furnished along with Table 2 and Fig-2

$E_{11}=120 \text{ GPa}, E_{22}= 7.9 \text{ GPa}, G_{12}= G_{23}=G_{13}=5.5 \text{ GPa}, \nu_{12}=0.30, \rho =1.58 \times 10^{-5} \text{ N-sec}^2/\text{cm}^4$  plate size=20cm

$.x \text{ 20cm. } x \text{ 0.269cm.};$  ply orientation =  $[ 0^\circ/45^\circ/0^\circ/-45^\circ/0^\circ]_s$  Velocity of impactor = 3m/s; Mass density of impactor =  $7.96 \times 10^{-5} \text{ N-sec/cm}^4$

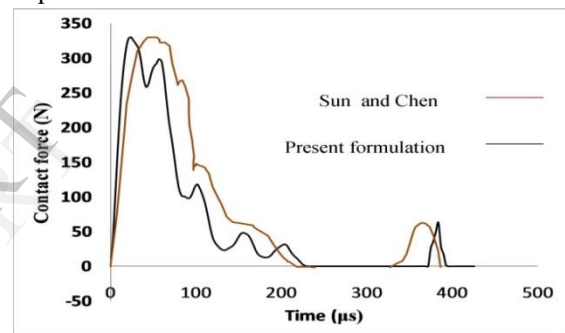


**Figure-2.**Contact force history of simply supported plate

Apart from the problems mentioned above, impact response of skewed hypar shells being impacted at the central point are also studied for point supported boundary condition for different impact velocities. The details of the problems which are the authors' own are given below.

- (i) Boundary condition :- Point supported (PS)
- (ii) Lamination:-  $+45^\circ/-45^\circ$  (AP)
- (iii) Velocity of impact (m/s):- 1, 3, 5, 10
- (iv) Details of shell geometry :  $a = 1.0\text{m}, b = 1.0\text{m}, t=0.02\text{m}, c=0.2\text{m}$
- (v) Material details :-  $E_{11}=120\text{Gpa}, E_{22}= 7.9 \text{ Pa}, G_{12}= G_{23}= G_{13}= 5.5\text{GPa}, \nu_{12} = 0.30, \rho = 1.58 \times 10^{-5} \text{ N-sec}^2/\text{cm}^4$

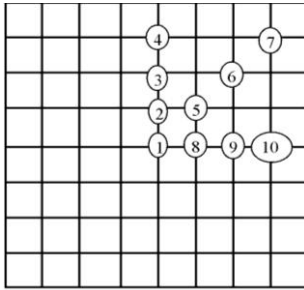


**Figure-3** Nodes at which deflections measured

#### 4. Results and discussions

The results of Table-1 shows that the fundamental frequency values of the twisted plates obtained by the present formulation for a shell with cross curvature agree very closely to those reported by Qatu and Lessia [14]. This agreement validates the correct incorporation of stiffness and mass matrix formulation in the present code. Fig.2 shows the time variation of the contact force induced in a composite plate under low velocity impact previously reported by Sun and Chen [3]. The values obtained by the present formulation are also presented graphically in the same figure in a different style. Here again excellent agreement of results is observed which establishes the correctness of impact formulation.

To study the impact response of point supported (PS) angle ply (AP) shell figure 5 to 8 and Table-2 are studied. All the results of contact force and displacement that are presented in either graphical or tabular form are arrived at after a study of time step convergence. The finite element mesh adopted is also based on force and displacement convergence criteria.

When low velocity normal impact response of simply supported angle ply shell is studied being struck by the spherical impactor centrally, it is observed that the contact force shows a sort of parabolic variation with a single peak. After a given time interval which is  $100\mu\text{s}$  or less the contact force converges to a null value. It is interesting to note that higher the impactor velocity higher is the contact force as expected, but the force dies down to a null value earlier. This behavior may be attributed to the fact that the higher the velocity more rapid is the elastic rebound of the impactor followed by detachment which causes contact force to decay out faster. It is also very interesting to observe that the time instant corresponding to peak contact force and that for peak displacement do not match. This is because the resultant displacement at any time instant is a cumulative effect of the instantaneous

contact force value and the inertia effect of the previous instant. The figure showing the transient displacement reflects the fact that vibration continues even after the force dies down with successively occurring peaks, though the peak values are less in magnitude than the highest peak which occurs a bit after the instant of maximum contact force but before the full decay of it.

To estimate the equivalent static load (ESL) corresponding to a particular impactor velocity, a concentrated load at the centre (point of impact) is applied and adjusted the yield a central displacement equal to the maximum dynamic displacement. The magnitude of the central displacement when the peak contact force is applied at the point of impact as a static concentrated load is also calculated. The central displacement obtained under such a load when divides the maximum dynamic displacements yields dynamic magnification factor (DMF). The variations of maximum contact force, maximum dynamic displacement and equivalent static load (ESL) with impactor velocity are almost linear and of three above mentioned values are increasing functions of impactor velocity (Fig-9). However the dynamic magnification factor (DMF) and the impactor velocity shows a logarithmic relation and the DMF is a decreasing function of the velocity of the impactor (Fig-9).

Apart from the central point displacements of some other points (Fig-3) are also calculated but the point of impact i.e. the central node is found to be the most critical one showing the highest magnitude of displacement.

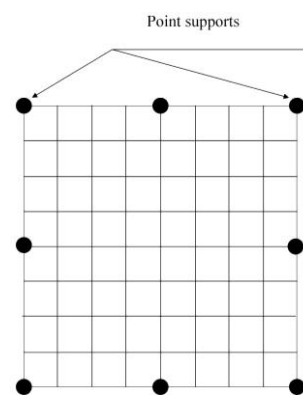


**Figure- 4** Position of point supports

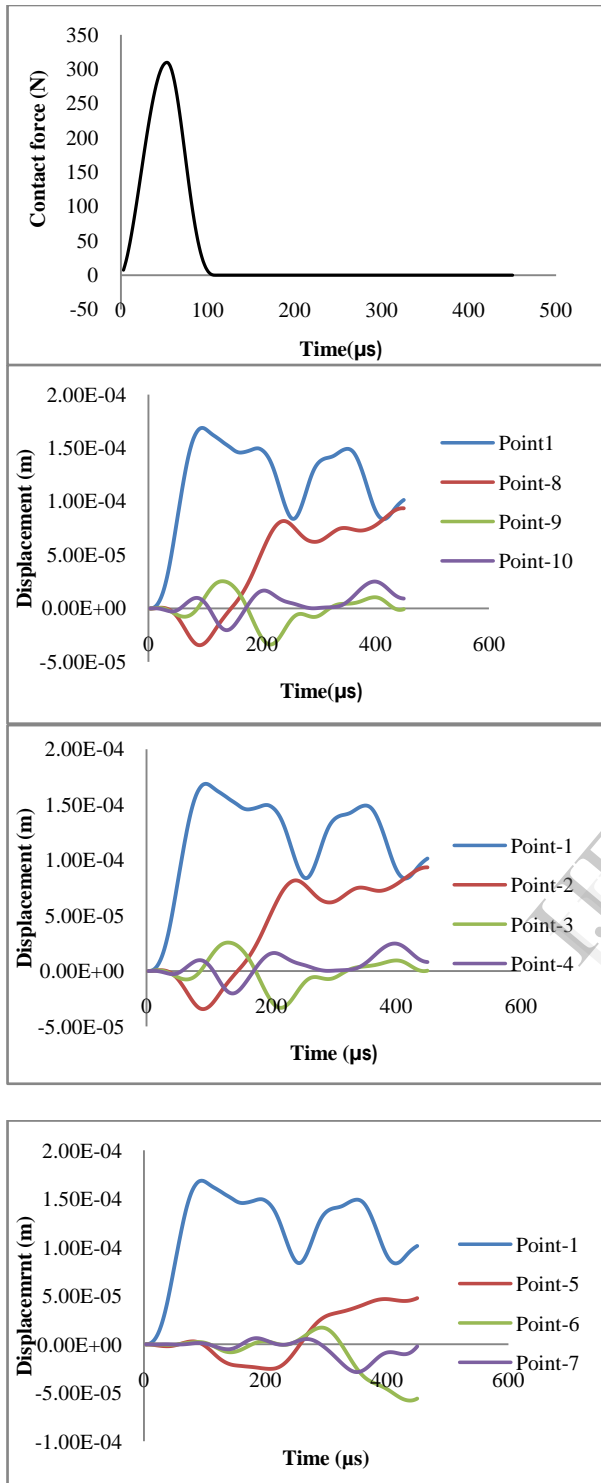


**Figure-5** Impact response of clamped angle ply (PS/AP) composite hyper shells for impact velocity 1m/s

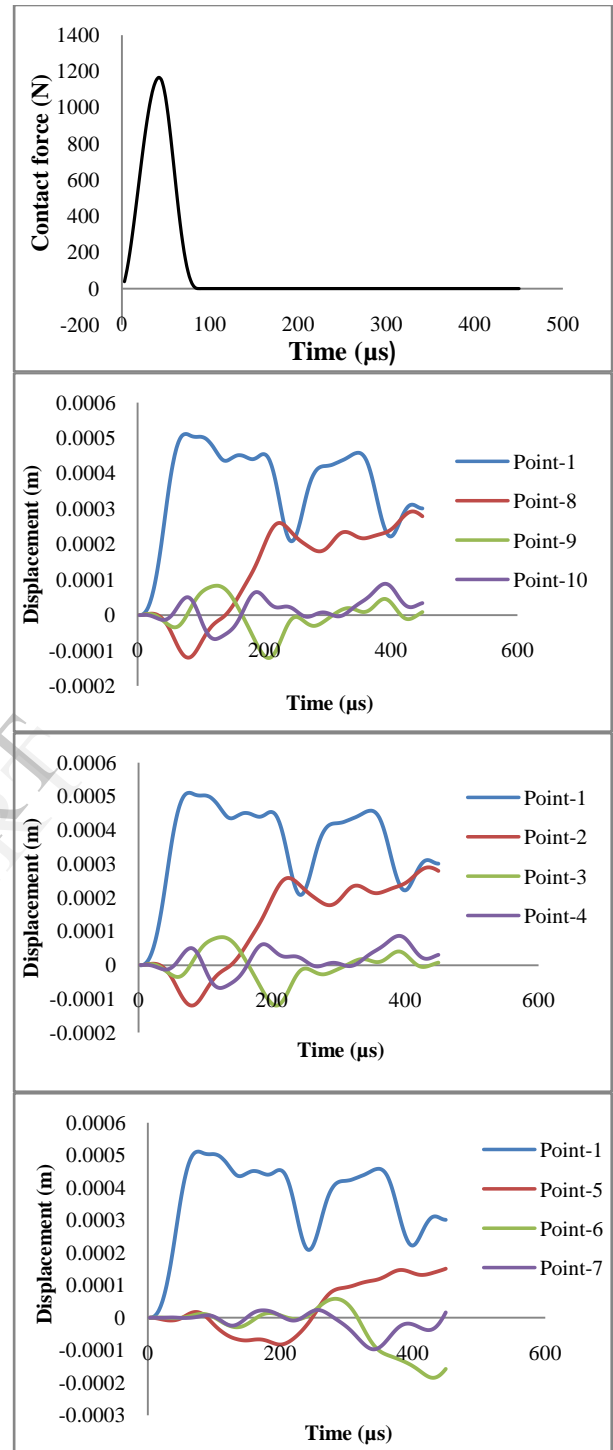


**Figure-6** Impact response of clamped angle ply (PS/AP) composite hyper shells for impact velocity 3m/s

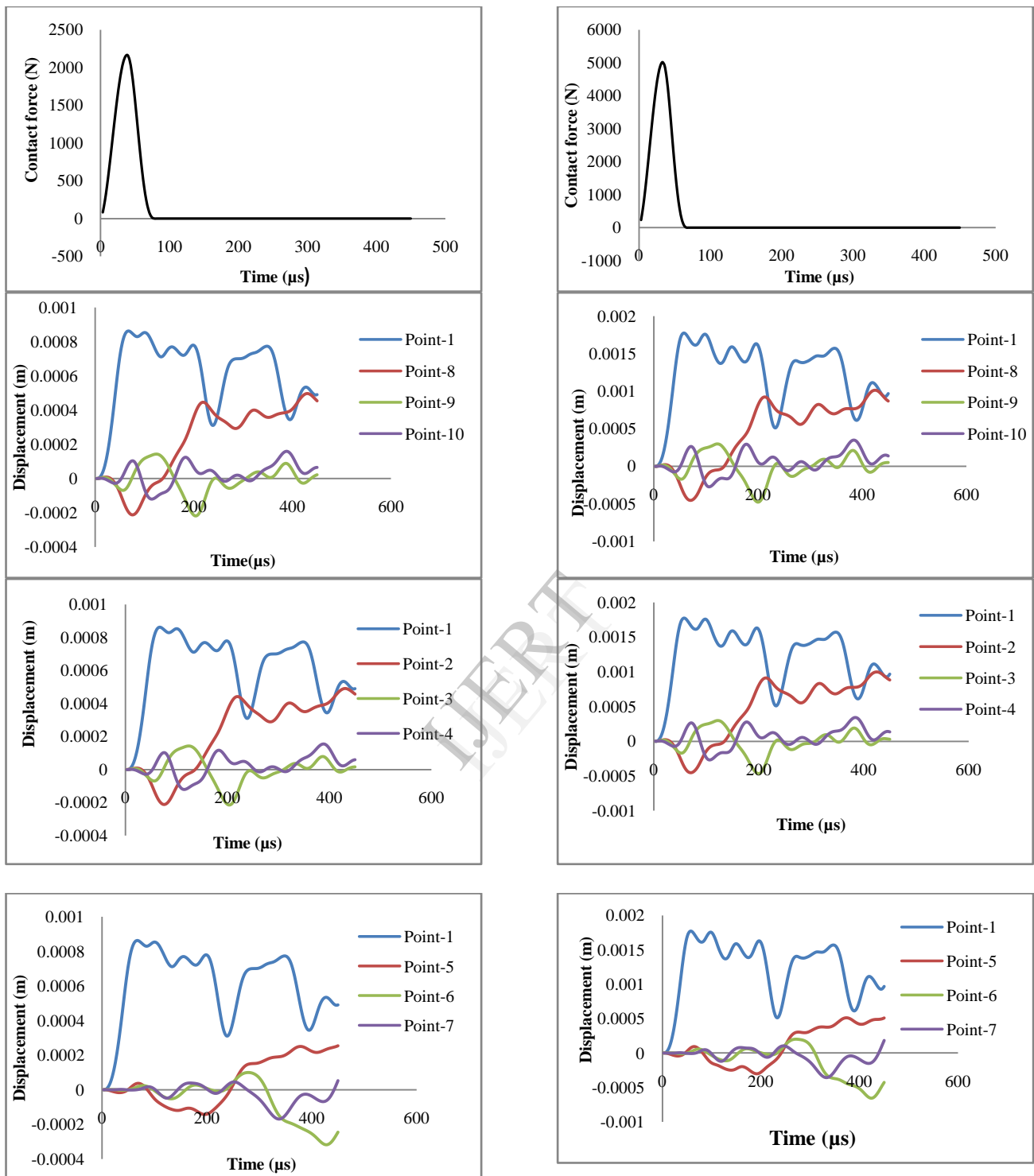


**Figure-7** Impact response of clamped angle ply (PS/AP) composite hyper shells for impact velocity 5m/s

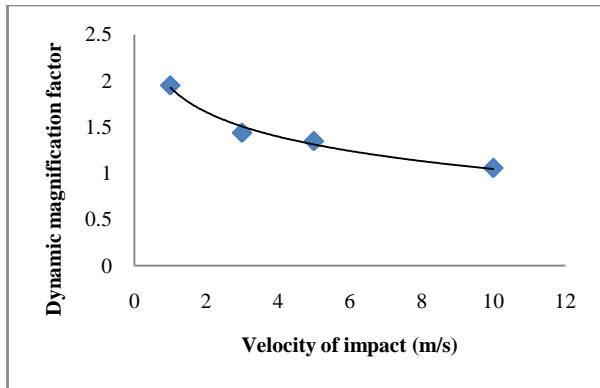


**Figure-9** Variation of dynamic magnification factor and equivalent static load with velocity for point supported cross ply (PS/CP) composite hypar

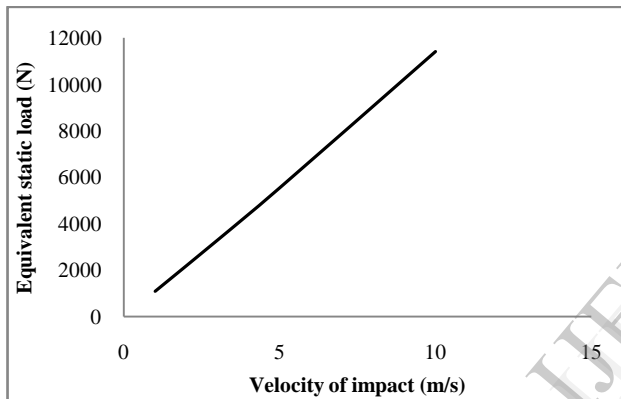


**Table- 2** Maximum contact force, maximum dynamic displacement, equivalent static load, dynamic magnification factor for different velocities

Boundary condition and ply orientation	Velocity(m/s)	Maximum impact load(N)	Maximum displacement(m)	Equivalent static load (N)	Dynamic magnification factor
Point-Supported +45 <sup>0</sup> /-45 <sup>0</sup>	1	309.4212	0.000169	1.089 x10 <sup>3</sup>	1.949
	3	1166.147	0.000511	3.292 x10 <sup>3</sup>	1.436
	5	2162.702	0.000861	5.547 x10 <sup>3</sup>	1.346
	10	5013.577	0.001772	11.416x10 <sup>3</sup>	1.055

## 5. Conclusion

The following conclusions may be derived from the present study.

1. The close agreement of the results obtained by the present method with those available in the published literature establishes the correctness of the approach used in the present investigation.
2. Under the influence of normal low velocity impact the contact force shows a parabolic combined loading and unloading curve with a single peak for the practical class of shells considered here. Higher magnitude of impact velocity results in higher value of the peak contact force. However, due to a sharp elastic rebound the total duration of contact force is less for higher velocity of impactor.
3. The time instants at which the maximum contact force and the maximum dynamic displacement occur show a phase difference and interestingly in some cases the maximum displacement and hence stresses may occur even after the contact force dies down totally. Thus it is concluded that the study should be continued only after when the major peaks of the dynamic displacement die down and not after the full decay of the contact force only.
4. The maximum contact force, the peak dynamic displacement and the equivalent static load are all increasing functions of impactor velocity, the relations being almost linear. However, the dynamic magnification factor shows a logarithmically decreasing tendency with increase of the velocity of impact

## 6. References

- [1] Hertz, H. On the contact of elastic solids, *Journal fur die reine und angewandte Mathematik*, (1881),92,156-171
- [2] Tan,T.M., Sun, C.T., Use of statical indentation laws in the impact analysis of laminated composite plate. *Journal of Applied Mechanics*. (1983),52,6-12
- [3] Sun, C.T., Chen, J.K., On the impact of initially stressed laminates, *Journal of Composite Material*. (1985), 19, 490-503
- [4] Toh S.L., Gong S.W., Shim V.P.W. Transient stress generated by low velocity impact on orthotropic laminated cylindrical shell, *Composite Structures*, (1995), 31(3),213-228
- [5] Shim, V.P.W., Toh S.L., Gong S.W., The elastic impact response of glass/epoxy laminated oval shells, *International journal of Impact Engineering*, (1996), 18(6) 633-655
- [6] Kistler, L.S., and Waas, A.M., Impact response of cylindrically curved including a large deformation scaling study, *International Journal of Impact Engineering*, (1998),21(1-2)61-75
- [7] Krishnamurthy K.S, Mahajan P, Mittal R.K, A parametric study of the impact response and damage of laminated cylindrical composite shells, *Composites Science and Technology*,(2001), 61(12) 1655-1669
- [8] Karmakar Amit, Kishimoto Kikuo Transient Dynamic Response of Delaminated Composite Cylindrical Shells Subjected to Low Velocity Impact, *Key Engineering Material*, (2005),297-300 1285-1290
- [9] Karmakar Amit, Kishimoto Kikuo Transient Dynamic Response of Delaminated Composite Rotating Shallow Shells Subjected to Low Velocity Impact, *Shock and Vibration*(2006), 13, 619-628.
- [10] Yiming Fu, Yiqi Mao, Yanping Tian Damage analysis and dynamic response of elasto-plastic laminated composite shallow spherical shell under low velocity impact, *International Journal of Solids and Structures*, (2009), 47 (1) 126–137
- [11] Sahoo, S .. Chakravorty, D., Finite element bending behaviour of composite hyperbolic paraboloidal shells with various edge conditions, *Journal of Strain Analysis for Engineering Design*, (2004), 39 (5) 499-513
- [12] Sahoo, S.. Chakravorty, D. Finite element vibration characteristics of composite hyper shallow shells with various edge supports, *Journal of Vibration and Control*, 2005,11(10) 1291-1309.
- [13] Das Neogi, S., Karmakar, A., Chakravorty, D. Impact response of simply supported skewed hyper shell roofs by finite element, *Journal of Reinforced Plastics Composites*. (2011), 30(21),1795-1805
- [14]Yang, S.H., Sun, C.T., Indentation law for composite laminates, *Composite Materials: Testing and Design, ASTM STP*(1985),787,425-446
- [15] Goldmith, W. IMPACT The theory and physical behavior of colliding solids, (2001), Dover Publication, Inc., New York,
- [16] Qatu, M. S., Leissa, A. W., Natural frequencies for cantilevered doubly-curved laminated composite shallow shells, *Computers and Structures*, (1991),17(3) 227-256



IJERT